

Off-axis properties of short gamma-ray bursts

H.-Th. Janka¹, M.-A. Aloy^{1,2}, P.A. Mazzali^{1,3}, and E. Pian^{1,3}

thj@mpa-garching.mpg.de

maa@mpa-garching.mpg.de

mazzali@mpa-garching.mpg.de

pian@ts.astro.it

ABSTRACT

Based on recent models of relativistic jet formation by thermal energy deposition around black hole-torus systems, the relation between the on- and off-axis appearance of short, hard gamma-ray bursts (GRBs) is discussed in terms of energetics, duration, average Lorentz factor, and probability of observation, assuming that the central engines are remnants of binary neutron star (NS+NS) or neutron star-black hole (NS+BH) mergers. As a consequence of the interaction with the torus matter at the jet basis and the subsequent expansion of the jets into an extremely low-density environment, the collimated ultrarelativistic outflows possess flat core profiles with only little variation of radially-averaged properties, and are bounded by very steep lateral edges. Owing to the rapid decrease of the isotropic-equivalent energy near the jet edges, the probability of observing the lateral, lower Lorentz factor wings is significantly reduced and most short GRBs should be seen with on-axis-like properties. Taking into account cosmological and viewing angle effects, theoretical predictions are made for the short-GRB distributions with redshift z , fluence, and isotropic-equivalent energy. The observational data for short bursts with determined redshifts are found to be compatible with the predictions only if either the intrinsic GRB rate density drops rapidly at $z \gtrsim 1$, or a large number of events at $z > 1$ are missed, implying that the subenergetic GRB 050509b was an extremely rare low-fluence event with detectable photon flux only because of its proximity and shortness. It appears

¹Max-Planck-Institut für Astrophysik, Karl-Schwarzschild-Str. 1, D-85741 Garching, Germany

²Departamento de Astronomía y Astrofísica, Universidad de Valencia, 46100 Burjassot, Spain

³Istituto Naz. di Astrofisica - OATs, Via Tiepolo, 11, I-34131 Trieste, Italy

unlikely that GRB 050509b can be explained as an off-axis event. The detection of short GRBs with small Lorentz factors is statistically disfavored, suggesting a possible reason for the absence of soft short bursts in the duration-hardness diagram.

Subject headings: gamma-ray bursts — hydrodynamics

1. Introduction

The origin of short GRBs has long been the subject of theoretical speculation. A long-standing prediction is that short GRBs might originate from NS+NS/BH mergers (e.g., Blinnikov et al. 1984; Paczyński 1986; Eichler et al. 1989; Mészáros 2002, and references therein). In the widely favored scenario a NS+NS/BH system gives rise to a BH girded by a dense torus of gas from the disrupted NS companion. The BH accretes mass at rates up to many solar masses per second, releasing huge amounts of gravitational binding energy mostly in neutrinos, gravitational waves, and through magnetohydrodynamic processes.

Hydrodynamic simulations (Aloy, Janka & Müller 2005; AJM05) show that thermal energy deposition around post-merger BH-torus systems, e.g., by neutrino-antineutrino annihilation, can drive collimated, ultrarelativistic outflows with the high Lorentz factors, internal variability and internal shocks that are deemed necessary to explain GRBs with the fireball model (e.g., Piran 2005). The collimation of observed short GRBs is rather uncertain and a matter of ongoing studies. Evidence for collimation was claimed in case of GRB 050709 (Fox et al. 2005), for which a jet semi-opening angle of $\theta_{\text{jet}} \sim 14^\circ$ was inferred. Although more observations are needed to confirm the collimation of short GRBs, this first indication seems to agree with the hydrodynamic simulations of AJM05. If the majority of short bursts has opening angles of that size, it would mean that only about 1% of all bursts point to Earth.

Only in the past year have a few short GRBs been localised. Their properties are recapped in Table 1. Two of these short GRBs are hosted by elliptical galaxies, and also the host galaxy of GRB 051221 appears to have a relatively evolved population of stars, despite its higher star-formation rate. This adds confidence to the idea that the progenitors of short GRBs are old systems. In addition, GRB 050509b is in the outskirts of its potential host, in agreement with expectations that coalescing compact binaries can travel large distances away from their birth sites during their long gravitational-wave driven inspiral (Tutukov & Yungelson 1994; Bloom, Sigurdsson, & Pols 1999). Moreover, a possible SN association has been ruled out for GRB 050509b (Hjorth et al. 2005; Castro-Tirado et al. 2005) and for GRB 050709 (Covino et al. 2005).

Three out of five short GRBs were detected at similar redshifts ($z \sim 0.2$), but their intrinsic isotropic-equivalent energy release in gamma rays, $E_{\gamma,\text{iso}}$, spans a factor of ~ 100 . The observation of intrinsically less energetic short GRBs at higher redshifts may be selected against.

In this paper we use the jet models of AJM05 to discuss theoretical predictions for the observable properties of short GRBs as a function of viewing angle (Sect. 2). In Sect. 3 we investigate the consequences of these models for the probability of observing short bursts with different isotropic equivalent energies and Lorentz factors, including the selection effects due to cosmological redshift. A summary and conclusions follow in Sect. 4.

2. Jets from post-merger black holes

By means of relativistic hydrodynamics simulations AJM05 studied the formation of ultrarelativistic outflows from BH-torus systems. The BH and torus masses and the deposition of thermal energy around the BH were chosen as expected from NS+NS/BH merger models. For different assumptions about the environment density and for varied geometry and time-dependence of the energy deposition rate, AJM05 followed the acceleration, collimation, and propagation of the ultrarelativistic outflows for an evolution time of 0.5 seconds. If the deposition rate of thermal energy per solid angle around the BH was sufficiently large, ultrarelativistic jets were launched along the rotation axis¹. Although these simulations are still far from taking into account all potentially relevant physics and did not self-consistently track the viscosity-driven torus evolution and its neutrino emission, they nevertheless provide useful insight into the conditions and properties of mass outflows from post-merger BH-torus systems.

The fact that an ultrarelativistic jet is launched from a “naked” BH-torus system has important consequences for its properties. While in the case of collapsars as sources of long GRBs the ultrarelativistic outflow originates from BH-torus systems at the center of a massive star, the polar jets in NS+NS/BH mergers do not have to plough through many solar masses of overlying stellar matter. Since the acceleration is not damped by swept-up matter, the jets very quickly reach Lorentz factors of a few. The acceleration is driven by the enormous radiation pressure of the pair-photon fireball produced by the energy release around the BH. Collimation of the baryon-poor jets is provided by the much denser torus

¹A lower limit to the energy deposition rate needed to drive a relativistic outflow is set by the fact that the ram pressure of polar mass infall to the BH must be overcome (see AJM05 for details; model B03 in that paper did not reach the energy deposition threshold and is therefore not considered here).

walls which gird the evacuated polar regions of the BH. As the jets propagate into the extremely low-density environment, they continue to accelerate, reaching maximum Lorentz factors of a few 100 within the simulated evolution time.

As a consequence of the interaction with the torus matter at the jet basis and the subsequent free expansion, the collimated ultrarelativistic outflows possess flat core profiles with only little variation of radially-averaged specific properties. These cores are bounded at their lateral edges by very steep gradients, which are not smoothed by the prolonged entrainment of baryons as in case of long GRB jets. The rapid decrease of the isotropic-equivalent energy as a function of θ implies, among other effects, that the probability of observing the lateral, lower Lorentz factor wings must be expected to be significantly reduced.

Figure 1 provides an overview of the hydrodynamics results for the sample of “type-B” models discussed by AJM05. In these simulations the BH-torus system was assumed to be surrounded by a very rarified medium. The models differ in the adopted rate of thermal energy deposition per solid angle and in the prescribed time dependence. The parameters were chosen such that the neutrino-antineutrino annihilation as calculated from NS+NS/BH merger simulations, and in particular for the post-merger accretion of a BH (Ruffert & Janka 1999; Janka et al. 1999; Janka & Ruffert 2002; Setiawan, Ruffert & Janka 2004), was qualitatively and quantitatively reproduced. Because of large variations of the torus masses expected from compact object mergers², AJM05 explored a variety of energy deposition properties, approximately covering the range of predictions from the above merger simulations (cf. Table 1 in AJM05).

The corresponding differences in the assumed energy deposition around the BH-torus systems account for the variation of the on-axis values of the *isotropic-equivalent kinetic plus internal energies*, $E_{\text{iso}}(\Gamma_{\infty})$, of jet matter with estimated terminal Lorentz factors $\Gamma_{\infty} > 100$ (Fig. 1, left). Γ_{∞} is estimated by assuming that 50% of the total specific energy will ultimately be converted to kinetic energy at large radii³. The models span a range of ~ 100 in E_{iso} , from some 10^{49} erg to several 10^{51} erg. Depending on the efficiency of energy conversion to γ -ray emission, the measurable γ -ray energy ($E_{\gamma,\text{iso}}$) may be roughly a factor of 10 lower than $E_{\text{iso}}(\Gamma_{\infty})$ (e.g., Guetta, Spada & Waxman 2001, and references therein). All models show a flat core and steep lateral wings in the radial average of Γ (Fig. 1, right), but models

²The mass of the remnant torus varies with the masses and spins of the binary components and with their mass ratio; it is also sensitive to still uncertain properties of dense NS matter and depends on general relativity effects that are included only in a subset of the current NS+NS/BH merger simulations.

³Note that an exact calculation of Γ_{∞} is beyond the scope of the hydrodynamic models of AJM05, because the simulations do not include physics that plays a role during the later stages of the jet acceleration.

B07 and B08 have a somewhat more shallow decline of E_{iso} because a gradual decrease of the energy deposition rate was assumed after an initial, burst-like phase. This caused a continuous decrease of the jet opening angle, thus softening the wings of the jet profile. It is currently not clear whether the jet-driving energy release of the BH-torus system follows such a burst/slow-decay behavior or whether it is powerful and roughly constant over a longer period of time before it ceases more abruptly, as assumed in the other models (B1–B6).

Figure 2 provides some observationally relevant quantities deduced from the hydrodynamics results. The profiles of $E_{\text{iso}}(\Gamma_\infty)$ given in the left panel there represent the isotropic-equivalent values of energy which is potentially radiated from the outflow in different directions. These profiles are calculated from the jet energies of Fig. 1, taking into account radiation contributions coming from regions outside of the line of sight. In order to compute these contributions, let us consider an amount of energy dE' that is radiated into the solid angle $d\Omega'$ at angle θ' relative to the direction of motion (primed quantities are measured in the local comoving frame). The transformation of the energy per solid angle between the comoving frame and the laboratory frame (e.g., a frame at rest with respect to the central BH) is (Rybicki & Lightman 1985)

$$\frac{dE}{d\Omega}(\theta) = \frac{1}{\Gamma^3(1 - \beta \cos \theta)^3} \frac{dE'}{d\Omega'} ,$$

where β is the velocity of the comoving frame as measured in the laboratory frame. Comparing the values of $\frac{dE}{d\Omega}$ at two different angles, $\theta = \theta_1$ and $\theta = 0$, one finds that the energy emitted per unit of solid angle around an angle θ_1 can be expressed in terms of the energy radiated along the direction of propagation ($\theta = 0$) as

$$\frac{dE}{d\Omega}(\theta_1) = \left(\frac{1 - \beta}{1 - \beta \cos \theta_1} \right)^3 \frac{dE}{d\Omega}(0) ,$$

if the radiation field is isotropic in the comoving frame. The emission from the jet in a certain observer direction θ_1 can now be obtained as the sum of the contributions from all matter moving in different directions with velocities β_0 at angles θ_0 relative to the jet axis, yielding

$$\left. \frac{dE}{d\Omega}(\theta_1) \right|_{\text{corr}} = \sum_{\theta_0} \left(\frac{1 - \beta_0}{1 - \beta_0 \cos(\theta_1 - \theta_0)} \right)^3 \frac{dE}{d\Omega}(\theta_0) . \quad (1)$$

Since the profiles of $E_{\text{iso}}(\theta)$ displayed in Fig. 1 are related to the energy radiated per unit solid angle into different directions $\theta = \theta_0$, the integration given in Eq. (1) can be directly applied to these profiles in order to obtain the isotropic equivalent energy distributions corrected for off-line-of-sight contributions. The results are plotted in Fig. 2. From the latter figure it is obvious that energy release with $E_{\text{iso}}(\Gamma_\infty) > 10^{48}$ erg is confined to semi-opening angles

between about 10° and 20° , corresponding to a collimation (“beaming”) factor of the two polar jets of $f_\Omega = 1 - \cos \theta_{\text{jet}}$ between 1.5% and 6%.

The relative observability of a short burst from a model of our set at different polar angles θ is shown in Fig. 2, middle panel. We plotted there the quantity

$$P(\theta) \equiv \frac{\sin \theta E_{\text{iso}}(\theta)}{\int_{-1}^1 d \cos \theta' E_{\text{iso}}(\theta')}, \quad (2)$$

where as a rough estimate for the detectability of a burst we assumed $f_{\text{det}}(\theta) \propto E_{\text{iso}}(\Gamma_\infty)$ (using for $E_{\text{iso}}(\Gamma_\infty)$ the data from the left panel in Fig. 2). The probability distribution confirms the steep lateral edges visible in the other quantities for models B01–B06 and the slightly softer wings in models B07 and B08, which correlate with a sharp drop of the average Lorentz factor. The probability $P(\theta)$ peaks at angles between 4° and $\sim 11^\circ$, which is a somewhat smaller range than that associated with $E_{\text{iso}}(\Gamma_\infty) > 10^{48}$ erg. Moreover, $P(\theta)$ nicely demonstrates the widening of the lateral visibility of a GRB with increasing energy deposition per solid angle around the BH (cf. the sequence of models B02, B04, B06, B01, and B05).

The hydrodynamic jet models of AJM05 track the formation of ultrarelativistic GRB-viable outflow. It turns out that the “shells” ejected by the central engine, i.e. the BH-torus system, accelerate much faster in the leading part of the outflow than the shells in its lagging part. The rear shells need therefore a longer time to reach velocities $v \approx c$. This different acceleration at early and late times of the relativistic wind ejection leads to a stretching of the overall radial length of the outflow, Δ , relative to the on-time t_{ce} of the central engine⁴ times the speed of light c , $\Delta > ct_{\text{ce}}$ (see Fig. 3). This stretching has the important consequence that the overall observable duration of the GRB (in the source frame), $T = t_\Delta = \Delta/c$, may be a factor of ten or more longer than the activity time of the central energy source (Fig. 3), even when the GRB is produced by internal shocks. This is only seemingly in conflict with the canonical fireball picture as discussed, e.g., by Piran (2005); Kobayashi, Piran & Sari (1997); Sari & Piran (1997); Nakar & Piran (2002), who draw the conclusion that “internal shocks continue as long as the source is active, thus the overall GRB duration T reflects the time that the inner engine is active”. It should in fact be noted that GRB light curve calculations in these shell collision models are based on the assumption that the shells move with *constant Lorentz factors and with a velocity very close to the speed of light*, which means that the expansion of the shells is considered only *after the preceding acceleration away from*

⁴We define the on-time or activity time of the central engine as the period of time during which the energy release of the BH-torus system is sufficiently powerful to drive an ultrarelativistic outflow as required for GRBs.

the central engine. Therefore the “shell emission time from the inner engine” (Piran 2005) or “ejection time” (Kobayashi, Piran & Sari 1997) or “activity time of the inner engine” (Nakar & Piran 2002) referred to in these works corresponds to the overall length the fireball has attained *in the saturated stage* after the initial acceleration. This time can only be identified with the real activity time or on-time of the central engine, whose energy output launches and drives the initial shell ejection, if the shells accelerate to nearly the speed of light within a negligibly small period of time. Only in this case the claim of equal emission and source activity times applies and can be traced back to the fact that a photon radiated from a fireball shell is observed almost simultaneously with a (hypothetical) photon launched at the central engine together with the radiating shell (Nakar & Piran 2002). The hydrodynamic jet simulations, however, show that the acceleration time, in particular for the shells ejected later, is not negligible (Fig. 3).

Taking the terminal length $\Delta(\theta)$ of the ultrarelativistic outflow in direction θ as a very crude measure of the overall observed duration $T(\theta)$ of a burst⁵, we have plotted this duration relative to the on-axis value in the right-hand panel of Fig. 2. The off-axis variations of the possible GRB durations are sizable. Bursts which are seen more than 5° – 10° off-axis have only 30%–60% of the on-axis duration. The outflow stretching can easily be the dominant effect determining the duration of short GRBs, but it is not possible to assess its relevance for long bursts without hydrodynamical modeling. This is due to the more complex and largely different dynamics of the collimated relativistic outflow caused by the presence of the massive star in the collapsar model.

Predictions of the absolute duration of the GRB emission based on jet simulations where the period of energy release was just a parameter are hard to make. Self-consistent torus evolution models, including the energy production mechanism and the feedback from jet formation, will be needed to provide reliable numbers for the duration of the source activity and the differential acceleration of the ejecta shells at early and late times. Moreover, the jet structure at 0.5 s after the jet creation, at which time AJM05 had to stop their calculations, may not be representative for the situation at the time when the GRB is produced.

⁵We estimate $\Delta(\theta)$ as the radial extension of those parts of the outflow which reach terminal Lorentz factors $\Gamma_\infty > 100$, where Γ_∞ of a mass element in the outflow is again calculated by assuming that 50% of its total energy will finally be converted to kinetic energy.

3. Predicted short GRB distributions

We can employ our set of jet models to attempt to predict the observable short-GRB distributions versus redshift z , fluence, isotropic equivalent energy output in γ -rays, $E_{\gamma,\text{iso}}$, and Lorentz factor Γ of the flow that produces the bulk of the measured γ -radiation. We discuss these aspects in view of the observed bursts of Table 1. Our methodology is different from that of other groups, who used observational data of GRB redshift, luminosity, and peak flux distributions to derive constraints on the intrinsic properties (event rates or lifetimes, jet collimation, luminosities) as functions of redshift (e.g., Ando 2004; Guetta & Piran 2005; Nakar, Gal-Yam & Fox 2005). We instead refer to the sample of jet models from AJM05 to define the intrinsic distribution of short GRB energies as a function of viewing angle for the individual events. This approach suffers from the huge uncertainties of the theoretical models (see below) and naturally can have only a tentative character.

In order to perform the analysis, we assume that our models have equal probability and are representative of the intrinsic variability of the short GRB source population at all redshifts. This is a crucial assumption and it can certainly be questioned, but currently it can hardly be replaced by more realistic alternatives, because the uncertainties concerning the link between NS+NS/BH binary parameters and GRB properties are still large.

In order to test the sensitivity of our analysis to a variation of the comoving short GRB rate density as function of redshift, $R_{\text{GRB}}(z)$, we consider three cases, namely an intrinsic GRB rate which (i) is constant with comoving volume, (ii) follows the star formation rate SF2–sfr of Eq. (4) in Guetta & Piran (2005), or (iii) varies according to the binary neutron star merger rate, case SF2+delay of Eq. (6) in Guetta & Piran (2005).

Based on these prescriptions, we produce the expected observable distributions of GRB properties by Monte Carlo sampling, randomly drawing GRB energies and Lorentz factors as functions of viewing angle θ from our set of GRB-jet models, using the results shown in Fig. 2 and Fig. 1, respectively. We estimate the isotropic-equivalent GRB energy output, $E_{\gamma,\text{iso}}(\theta)$, by reducing the isotropic equivalent kinetic plus internal energy of the outflow, $E_{\text{iso}}(\theta)$ of Fig. 2, by a factor of 10. This is supposed to account for the limited efficiency of energy conversion to γ -rays and the fact that only a fraction of the γ -emission occurs in the energy band of a measurement⁶. Our set of models can be considered to define a co-moving space distribution function $\tilde{\Phi}(\theta, E_{\gamma,\text{iso}}, \Gamma)$, which is assumed to be normalized to unity and whose integral over Γ yields another normalized distribution function, $\Phi(\theta, E_{\gamma,\text{iso}}) \equiv \int d\Gamma \tilde{\Phi}$.

⁶A careful inclusion of a redshift-dependent k-correction appears inappropriate, because we do not apply detailed theoretical arguments to estimate the conversion efficiency of jet energy to γ -radiation, and model-dependent spectral properties of the γ -ray emission are disregarded as well.

The random angle between the jet axis and the line of sight is denoted by θ . Formally, the expected redshift distribution of measured bursts can be computed from the intrinsic distribution as

$$\dot{N}(z_1, z_2) = \int_{z_1}^{z_2} dz \frac{dV}{dz} \frac{R_{\text{GRB}}(z)}{1+z} \int_{-1}^{+1} d\mu 2\pi \int_{E_{\gamma,\text{iso}}^{\text{min}}(\theta, f_{\text{min}}, z)}^{E_{\gamma,\text{iso}}^{\text{max}}(\theta)} dE \Phi(\theta, E), \quad (3)$$

when $\dot{N}(z_1, z_2)$ represents the observed rate of events in the redshift interval $z_1 < z < z_2$ (in the following we will only consider normalized distributions and the absolute value of the rate will be of no concern). In Eq. (3), $\mu = \cos \theta$, $dV/dz = 4\pi D_L^2(z) c [H_0(1+z)^2 (\Omega_M(1+z)^3 + \Omega_K(1+z)^2 + \Omega_\Lambda)^{1/2}]^{-1}$ is the comoving volume element, and $(1+z)^{-1}$ accounts for cosmological time dilation. The cosmological parameters used in our study are $H_0 = 72 \text{ km s}^{-1} \text{ Mpc}^{-1}$, $\Omega_\Lambda = 0.72$, $\Omega_M = 0.28$, and $\Omega_K = 1 - \Omega_M - \Omega_\Lambda$. In Eq. (3) as well as in Eqs. (4)–(6) below, an instrument specific detection probability that depends on the photon flux and thus on the burst luminosity, spectrum, and redshift, is ignored (we have no information on this quantity in terms of the fluence). $E_{\gamma,\text{iso}}^{\text{min}}(\theta, f_{\text{min}}, z)$ is the isotropic equivalent energy corresponding to the minimum fluence f_{min} that can be measured by the detector, and $E_{\gamma,\text{iso}}^{\text{max}}(\theta)$ corresponds to the maximum energy release of the models of our sample in a certain direction θ . The fluence at the instrument is computed from the intrinsic energy output $E_{\gamma,\text{iso}}(\theta)$ (in the reference frame of the source) and from the luminosity distance $D_L(z)$ as $f(\theta, z) = (1+z) E_{\gamma,\text{iso}}(\theta) / [4\pi D_L^2(z)]$.

The predicted distribution of Lorentz factors of the observed bursts can be written as

$$\dot{N}(\Gamma_1, \Gamma_2) = \int_{-1}^{+1} d\mu 2\pi \int_{\Gamma_1}^{\Gamma_2} d\Gamma \int dE_{\gamma,\text{iso}} \tilde{\Phi}(\theta, E_{\gamma,\text{iso}}, \Gamma) \int_0^{z_{\text{max}}(E_{\gamma,\text{iso}}(\theta), f_{\text{min}})} dz \frac{dV}{dz} \frac{R_{\text{GRB}}(z)}{1+z}, \quad (4)$$

where $z_{\text{max}}(E_{\gamma,\text{iso}}(\theta), f_{\text{min}})$ is the maximum redshift at which GRBs with isotropic equivalent energy $E_{\gamma,\text{iso}}(\theta)$ produce a fluence above the lower detection bound f_{min} . Similarly, the fluence distribution is given by

$$\dot{N}(f_1, f_2) = \int_{-1}^{+1} d\mu 2\pi \int_0^\infty dz \frac{dV}{dz} \frac{R_{\text{GRB}}(z)}{1+z} \int_{E_{\gamma,\text{iso}}(f_1(z))}^{E_{\gamma,\text{iso}}(f_2(z))} dE \Phi(\theta, E) \quad (5)$$

with $f_2 > f_1 \geq f_{\text{min}}$, when $E_{\gamma,\text{iso}}(f_1(z))$ and $E_{\gamma,\text{iso}}(f_2(z))$ are the isotropic equivalent energies of γ -radiation that account for fluences f_1 and f_2 in the frequency window of the detector

for a GRB at redshift z . The distribution versus $E_{\gamma,\text{iso}}$ can be represented by

$$\dot{N}(E_{\gamma,\text{iso}}^1, E_{\gamma,\text{iso}}^2) = \int_{-1}^{+1} d\mu 2\pi \int_{E_{\gamma,\text{iso}}^1}^{E_{\gamma,\text{iso}}^2} dE_{\gamma,\text{iso}} \Phi(\theta, E_{\gamma,\text{iso}}) \int_0^{z_{\text{max}}(E_{\gamma,\text{iso}}(\theta), f_{\text{min}})} dz \frac{dV}{dz} \frac{R_{\text{GRB}}(z)}{1+z}. \quad (6)$$

We perform our investigation with two different values of the lower fluence cutoff for detection (i.e., the detection threshold is assumed to be a step function). For one simulation we use $f_{\text{min}} = 10^{-8} \text{ erg cm}^{-2}$, which corresponds to the fluence of the very weak GRB 050509b and thus can be considered as a lower bound of the sensitivity of Swift. In a second simulation we use a cutoff value of $f_{\text{min}} = 1.6 \times 10^{-7} \text{ erg cm}^{-2}$, which we derive from the limiting flux, $\phi_{\text{min}} = f_{\text{min}} / [(1+z)T_i \epsilon_\gamma]$, of 1 photon $\text{cm}^{-2} \text{s}^{-1}$ adopted for the BATSE instrument by Guetta & Piran (2005), making the assumption that $(1+z)T_i \epsilon_\gamma = 100 \text{ keV s}$ is a representative value for the product of photon detection time interval and energy (T_i is the intrinsic duration of the burst). This higher fluence threshold seems to be compatible with the sample of (bright) BATSE bursts listed in Table 1 of Ghirlanda, Ghisellini & Celotti (2004). We note that Nakar et al. (2005) employ a detection threshold of 1 photon $\text{cm}^{-2} \text{s}^{-1}$ also for Swift. A higher value for f_{min} may further be motivated by the fact that the photon flux decreases with increasing redshift more rapidly than the fluence by an additional factor $(1+z)^{-1}$. Therefore a low fluence threshold for detection may overestimate the number of high- z events observed.

To obtain normalized distributions, $\dot{N}(x_1, x_2) / \dot{N}$, we do not evaluate the integrals in Eqs. (3)–(6) directly, but perform Monte Carlo sampling of a large number of GRB events at different redshifts, with random orientations and with properties drawn randomly from the model data plotted in Figs. 1 and 2, thus constructing the discrete distribution functions $\tilde{\Phi}$ and Φ which describe the GRB properties according to our set of jet simulations. The sampled events with $f \geq f_{\text{min}}$ are then collected into bins to build up the normalized probability distributions versus redshift, fluence, $E_{\gamma,\text{iso}}$, and Γ shown in Fig. 4. We point out that the Lorentz factors are based on those of Fig. 1 and therefore reflect the situation only 0.5 s after the ejection of relativistically expanding matter. Because of subsequent acceleration and conversion of internal to kinetic energy (which we are unable to trace in the hydrodynamic simulations), the terminal values Γ_∞ must be expected to be larger by a factor of 2–3.

Our predictions for the observable distributions vs. redshift, fluence, energy, and Lorentz factor for the two chosen values of the fluence cutoff are displayed in Fig. 4. The corresponding locations of four of the five bursts listed in Table 1 are also indicated. The very bright short GRB 051221 is outside of the energy scale of the third panel, hence we omitted it from Fig. 4. This burst is too energetic to be accounted for by the range of γ -burst energies considered in our set of jet models, in which we assumed that 10% of the ejecta energy can

be converted to radiation in the frequency band of the measurement. But if this fraction were significantly higher — the observations of GRB 051221 indeed suggest a total efficiency of 60–70% (Soderberg et al. 2006) — then the output of γ -energy of this burst would be within the reach of our models for near-axis observation (cf. Fig. 1). Our jet models invoked energy deposition rates as obtained for the annihilation of neutrino-antineutrino pairs in NS+NS/BH merger and post-merger accretion simulations (for details and references to original work, see AJM05). We therefore conclude that GRB 051221, if it is indeed located at a redshift of 0.546, does not make a strong case for different underlying energy extraction mechanisms (e.g., magnetohydrodynamic processes) and/or different progenitors as speculated by Soderberg et al. (2006).

It is obvious that the choice of the lower fluence cutoff has a big impact on the redshift distribution (left panels). For a detection threshold of 10^{-8} erg cm $^{-2}$ and our employed co-moving GRB rate densities, the majority of bursts should be seen at redshifts $z > 1$, while with the higher cutoff we predict that bursts with $z > 0.75$ would not be detected. Clearly, the observations of the recent bursts with redshifts between 0.16 and 0.72 are more compatible with the latter case. At the request of one referee, we performed a Kolmogorov-Smirnov (KS) test (not including the very energetic GRB 051221), which gives significance levels of 5%, 8%, and 20% for the consistency of the observations with the theoretical distributions for the three tested GRB rate densities SF2–sfr, SF2+delay, and “constant”, respectively (the KS probabilities in case of the lower cutoff value are 0.1%, 0.4% and 2%). Better agreement is therefore found when the simulation predicts a larger number of nearby events. Highest preference is attributed to the constant GRB rate density, in which the relative fraction of visible bursts at $z < 0.5$ is largest. This is in qualitative agreement with the recent analysis by Nakar et al. (2005; see Fig. 5 there), who found that the well-localized bursts imply a high local rate of short-hard GRBs events, and that long lifetimes of the progenitor systems are favored. Given the small number of events, the results clearly will change significantly with every new observation (see Bloom & Prochaska 2006).

The fluence distributions show the expected increase towards faint events, and the distribution of $E_{\gamma,\text{iso}}$ reveals a strong bias towards events with higher isotropic-equivalent energies, corresponding to near-axis observation. Such events are much more likely to yield a fluence above the threshold values at large redshifts and are also preferred because of the steepness of the jet wings, which reduces the probability of seeing events from those wings. GRB 050509b is an exceptionally weak event, which is well separated from the other observed bursts, and which the theoretical distributions do not account for. It thus distorts the KS measures for the fluence and energy distributions, which otherwise signal reasonably good compatibility between calculations and observations, in particular for the higher fluence threshold. GRB 050509b is most probably *not* an off-axis observation, but requires either an event

with lower energy output than for any of the jet models in our sample, or an efficiency of the energy conversion to γ -rays lower than assumed here. The latter is disfavored by the observations of Bloom et al. (2005). These authors also discard GRB 050509b as an off-axis event on the basis of the very early decay of the afterglow light curve.

The probability distribution of the Lorentz factor reflects the discreteness of our sample of models, because the redshift has no influence on Γ and because the jet wings are extremely steep and the off-axis visibility much reduced (see Fig. 1). Therefore, the high-energy model B05 with a relatively wide jet clearly sticks out in the Γ -distribution. A continuous set of models would enhance and broaden this peak, and the “underwood” of events extending to low values of Γ would even be more reduced if terminal Lorentz factors Γ_∞ instead of Γ were plotted.

We hypothesize that this clear bias towards observing high- Γ events may be connected with the lack of short-soft GRBs in the duration-hardness diagram. Short bursts are on average harder than long bursts, and short-soft bursts are rare or missing, because short GRBs develop jets with higher Lorentz factors and very steep edges. The underlying reason behind this effect is the fact that jets from post-merger BH-torus systems do not have to make their way out of a massive star through layers of dense stellar material, which can damp the outflow acceleration by mass entrainment. In the commonly used internal shock scenario for the GRB emission the peak energy of the (synchrotron) spectrum, E_p , obeys the relation $E_p \propto \Gamma^b$ with $b \sim -2$ (e.g., Daigne & Mochkovitch 2003; Ramirez-Ruiz & Lloyd-Ronning 2002; Zhang & Mészáros 2002). In view of our jet models this would imply that short bursts might have lower E_p but nevertheless be harder than long ones because of a steeper increase of the νF_ν spectrum below the peak. The results of Ghirlanda et al. (2004) seem to confirm this. Their spectral analysis for a sample of short bright GRBs detected by BATSE in comparison with the spectral properties of long bright BATSE bursts indeed reveals a significantly harder (i.e., less negative) spectral index α rather than a larger peak energy E_p for short GRBs. This leads to an increased hardness ratio if E_p is above the higher energy band of the spectral hardness measure, or overlaps with it, which is the case for almost all of the short GRBs listed in Table 1 of Ghirlanda et al. (2004). We point out that the difference between the peak spectral energies of short and long bursts might even be more pronounced than found by Ghirlanda et al. (2004) if long bursts occurred at typically higher redshifts and the intrinsic values of these energies were compared.

However, the discussion by Zhang & Mészáros (2002) also leaves possibilities how in the internal shock model higher Lorentz factors of short GRBs may be compatible with *higher* peak spectral energies. In case of Poynting-flux dominated outflow, Zhang & Mészáros (2002) expect a direct proportionality, $E_p \propto \Gamma$ (see their Eq. 21 and case (b) in their

Fig. 3), and for a kinetic-energy dominated fireball they find $E_p \propto L^{1/2} R_{\text{int}}^{-1}$ (see their Eq. 17) when $R_{\text{int}} \approx \Gamma^2 c \delta t$ is the radius where internal shock collisions produce γ -ray emission (see, e.g., Piran 2005). Although short GRBs have higher Γ 's compared with long GRBs, their variability timescale δt might be generically much smaller. This would result in a smaller shock dissipation radius and therefore in a higher E_p , because magnetic fields may be stronger at a smaller radius.

4. Discussion and Conclusions

Using a set of hydrodynamic simulations of ultrarelativistic jet formation by thermal energy release around BH-torus systems as remnants of NS+NS/BH mergers (AJM05), we have investigated the off-axis visibility of short GRBs produced by such outflows. The jets are characterized by narrow cores with high isotropic-equivalent energies and very high Lorentz factors, which are laterally bounded by steep wings. These properties are a consequence of the specific conditions in which the jets are considered to be launched, i.e., their acceleration away from the torus-girded BH, where the energy is released, into an environment of extremely low density. The observability of short GRBs is therefore strongly favored within a cone of semi-opening angle between about 10° and 15° around the jet axis.

We argued that the observable duration of short GRBs both in the external shock model and in the internal shock collision model for GRB production can be significantly longer than the activity time of the central engine whose energy release powers the GRB-visible ultrarelativistic outflow. The reason for this claim is the fact that our jet formation simulations showed that during the acceleration phase the fireball experiences significant radial stretching, because hydrodynamic effects cause the acceleration to proceed differently in the leading and lagging parts of the outflow. Therefore the overall radial length Δ of the relativistic ejecta can become a factor of ten or more larger than $c t_{\text{ce}}$, when t_{ce} is the on-time of the central engine (Fig. 3). This seems to be in conflict with the canonical internal shock scenario, according to which the observed GRB is produced by shell collisions such that the observed light curve reflects the temporal activity and overall duration of the energy release by the “inner engine” (Piran 2005). However, the standard picture applies only if the fireball shells move immediately after their ejection with velocities that are very similar (but not necessarily identical) and very close to the speed of light. This can be traced back to the fact that a photon radiated from a fireball shell is observed almost simultaneously with a (hypothetical) photon emitted from the central engine together with the radiating shell (Nakar & Piran 2002). If the acceleration is differential, and in particular if the acceleration of shells ejected by the central engine at later times proceeds more slowly, the fireball evolution

after creation at the engine is more complex (Fig. 3). Its emission pattern then does not directly replicate the activity timescales and the on-time of the central source.

In order to investigate the consequences of the reduced off-axis visibility of short GRBs produced by our jets, we made an attempt to predict observable short-hard GRB distributions with redshift, fluence, isotropic-equivalent energy, and Lorentz factor. For this purpose we made use of a sample of seven ultrarelativistic jet models (AJM05), which roughly covers the range of energy release expected from neutrino-antineutrino annihilation in NS+NS/BH binary mergers. Employing these models for defining the intrinsic GRB properties, we performed a Monte Carlo sampling of the expected observed event distributions. Our analysis took into account the off-axis variation of the jet properties as provided by the hydrodynamic simulations (Figs. 1 and 2) and referred to standard prescriptions for the intrinsic event rate density as a function of redshift (constant rate as well as the cases SF2–sfr and SF2+delay from Guetta & Piran 2005). We found that the resulting distributions predict far too many bursts at $z > 1$ and therefore show no good agreement with the recent observations when a fluence threshold of $10^{-8} \text{ erg cm}^{-2}$ as suggested by GRB 050509b was adopted (the KS probability for the observed and predicted data being drawn from the same distribution is less than 1%). Improved consistency was achieved when we performed our analysis with a higher fluence threshold of $1.6 \times 10^{-7} \text{ erg cm}^{-2}$. In this case the bursts at $z \gtrsim 0.8$ escape from observation and the KS significance increases to $\sim 20\%$ for the constant comoving GRB rate density. This would imply that GRB 050509b was a very special and extremely rare case with an exceptionally low fluence, which due to its shortness and proximity still had a sufficiently large photon flux of about $1 \text{ photon s}^{-1} \text{ cm}^{-2}$ and was therefore above the Swift detection threshold. Comparison of the results for different comoving GRB rate densities revealed that the consistency between theory and observations increases when the rate yields a relatively larger number of events at redshifts $z \lesssim 0.5$ rather than an increase for higher values of z . Our results agree qualitatively with those of Nakar et al. (2005), who found that the detection of the current sample of low- z short GRBs is best compatible with a very low comoving rate density for $z > 1$ and a peak at $z \lesssim 0.5$.

The extremely weak GRB 050509b is clearly separated in energy from the other observed events and cannot be accounted for by off-axis observation of any of the modelled jet outflows. It seems to require an intrinsically less energetic event, because an efficiency of energy conversion to γ -rays significantly lower than what we used is disfavored by observations (Bloom et al. 2005). On the other hand, the very energetic GRB 051221 exceeds the isotropic-equivalent GRB energies predicted by our jet models, making the assumption that 10% of the ejecta energy can be converted to radiation in the detector frequency band. If, however, this fraction is as high as suggested by the measurements (60–70% for the total efficiency in case of GRB 051221; Soderberg et al. 2006) and GRB 051221 happened indeed

at a redshift of 0.546 and not farther away, then this strong burst is also within the reach of the most energetic one of our models if observed near-axis. Therefore we do not think that GRB 051221 gives strong support to speculations that different progenitors and/or different energy extraction mechanisms than neutrino-antineutrino annihilation are needed to explain the observed large spread in short burst energies and the high energy of GRB 051221 in particular (Soderberg et al. 2006).

Because of the steep wings of the jet profiles in both isotropic-equivalent energy and Lorentz factor Γ , our analysis reveals a clear bias towards the detection of short GRBs with high Γ values. Since higher Lorentz factors and steep jet edges may be characteristic features of GRB jets that originate from post-merger BH-torus systems, which makes them different from collapsar jets, we propose that they are the reason why short GRBs are typically harder than long ones. In the internal shock scenario for GRB emission, this might imply that the peak energy of the synchrotron spectrum is lower ($E_p \propto R_{\text{int}}^{-1} \propto \Gamma^{-2} \delta t^{-1}$). Short bursts could therefore be harder not because of a higher E_p but because of a steeper increase of their νF_ν spectra below the peak energy. This would require the spectral maximum to lie above or inside the high-energy band for the hardness ratio. Such properties were indeed concluded from a spectral analysis of a sample of short bright BATSE GRBs in comparison with long burst spectra (Ghirlanda et al. 2004). Alternatively, a higher Γ could still allow for a larger E_p if the variability timescale δt of short GRBs were generically much smaller than that of long GRBs.

We point out that our exploration can only be tentative. Both the theoretical models and observational data still involve large uncertainties, which have an impact on our analysis. Not only did we take a very simplistic approach in estimating the γ -ray production of our jet models in the energy band of the detector. We just assumed that a fraction of 10% of the ejecta energy is converted to γ -emission at the relevant frequencies. We also did not account in detail for the instrument specific detection probability that depends on the photon flux and thus on the burst luminosity, spectrum, and redshift, but simply assumed that all short GRBs above a certain fluence threshold are detected, independent of their peak luminosity and spectral properties. Moreover, the intrinsic short GRB rate per unit of comoving time and comoving volume enters the analysis sensitively. Nakar et al. (2005) found that the well-localized short GRBs, which are all at $z < 1$, require a very large number of nearby events. This implies that the local number density of double neutron star binaries or neutron star-black hole systems is significantly above previous estimates, if short GRBs come from such objects. In fact, it must be dominated by a so far undetected old population of double neutron stars or, alternatively, by observationally unconstrained NS+BH systems. A caveat of such conclusions and of comparisons to the observations is, of course, the still very small sample of well-localized short GRBs. Caution is therefore advisable until the

empirical foundation is more solid (see Bloom & Prochaska 2006).

We restricted our analysis to the properties of the prompt emission of short GRBs, which may originate from neutrino-annihilation driven hydrodynamic jets, launched by the neutrino energy release of a hyperaccreting BH girded by a massive torus. Of course, one cannot exclude that magnetohydrodynamic effects might play a role that deserves more theoretical exploration. The discovery of X-ray flares following the short-duration, hard pulse of GRB 050724 after hundreds of seconds (Barthelmy et al. 2005) was interpreted as observational hint for the importance of such magnetic processes (Fan, Zhang, & Proga 2005). If these late-time X-ray flares are indeed connected with an extended period of activity or a restart of the central engine long after the prompt emission is over (Burrows et al. 2005, Zhang et al. 2005, Liang et al. 2006), it seems not possible to explain these late outbursts by the accretion-rate dependent neutrino mechanism (Fan, Zhang, & Proga 2005). A prompt phase of neutrino (or neutrino plus magnetic) energy release that creates the short-hard GRB may thus be followed by a much more extended period of reduced source activity, in which X-ray flares could be powered by a magnetic mechanism (Fan et al. 2005).

Admittedly, our investigation of the implications of the off-axis properties of short GRB jets from post-merger BH-torus systems was also based on a very limited set of numerical models (AJM05). This theory input of our analysis replaces the intrinsic peak luminosity function based on measured data used in other works (e.g., Nakar et al. 2005, Guetta & Piran 2005). The models were chosen to span approximately the possible diversity of the properties of ultrarelativistic outflows from such systems, but certainly represent it only incompletely. In particular, they were calculated with a single setup for the BH-torus system, in which the deposition rate of thermal energy and its spatial distribution (expressed in terms of the opening angle of the axial cone of the main energy deposition) was varied over a range guided by the results for neutrino-antineutrino annihilation in independent binary merger and post-merger evolution models. Neither was the torus evolved self-consistently in response to this energy release and to the jet formation, nor were magnetohydrodynamic effects included in the models. There is still a long way to go before the challenging problem of fully consistent modeling becomes manageable. This should include all relevant physics and track in full general relativity the history from the last orbits of the pre-merging binary, through the merging phase, to the possible BH formation and the subsequent secular post-merging evolution of the accreting relic black hole. Such simulations will ultimately have to be performed for a carefully selected sample of progenitor systems, which avoids the “arbitrariness” of the variations in our current set of models. Knowing that this goal is still far ahead and in view of the fact that the simulations available to us represent the present state-of-the-art of modeling collimated relativistic outflows from post-merger BH-torus systems, we tried to explore how far this information can help us bridging GRB engine

theory and observations.

Stimulating discussions with Shri Kulkarni and Elena Rossi and help by Leonhard Scheck with Fig. 4 are acknowledged. We are very grateful to anonymous referees for their very interesting comments, which led to significant improvements of our manuscript. The project was supported by SFB 375 “Astroparticle Physics” and SFB-TR 7 “Gravitational Wave Astronomy” of the Deutsche Forschungsgemeinschaft, and by the RTN program HPRN-CT-2002-00294 “Gamma-Ray Bursts: an Enigma and a Tool”. MAA is a Ramón y Cajal Fellow of the Spanish Ministry of Education and Science and is grateful for partial support of the Spanish Ministerio de Ciencia y Tecnología (AYA2001-3490-C02-C01).

REFERENCES

- Aloy, M. A., Janka, H.-T., Müller, E. 2005, *A&A*, 436, 273 (AJM05)
- Ando, S. 2004, *JCAP*, 06, 007
- Barthelmy, S.D., et al. 2005, *Nature*, 438, 994
- Berger, E., Price, P. A., et al. 2005, *Nature*, 438, 988
- Blinnikov, S.I., Novikov, I.D., Perevodchikova, T.V., & Polnarev, A.G. 1984, *Soviet Ast. Lett.*, 10, 177
- Bloom, J.S. & Prochaska, J.X., in *Proc. 16th Annual October Astrophysics Conference in Maryland, “Gamma Ray Bursts in the Swift Era”*, eds. S. Holt, N. Gehrels and J. Nousek (astro-ph/0602058)
- Bloom, J.S., Sigurdsson, S., Pols, O.R., 1999, *MNRAS*, 305, 763
- Bloom, J.S., et al. 2001, *AJ*, 121, 2879
- Bloom, J.S., et al. 2006, *ApJ*, 638, 354
- Boer, M., et al. 2005, *GCN Circular N.* 3653
- Burrows, D.N., et al. 2005, *Science*, 309, 1833
- Castro-Tirado, A., et al. 2005, *A&A*, 439, L15
- Covino, S., Malesani, D., et al. , 2005, *A&A*, 447, L5

- Daigne, F., Mochkovitch, R., 2003, MNRAS, 342, 587
- Eichler, D., Livio, M., Piran, T., & Schramm, D. N. 1989, Nature, 340, 126
- Fan, Y.Z., Zhang, B., Proga, D. 2005, ApJ, 635, L129
- Foley, R.J., et al. 2005, GCN Circular N. 3808
- Fox, D. B., et al. 2005, Nature, 437, 845
- Gehrels, N., et al. 2005, Nature, 437, 851
- Guetta, D., & Piran, T. 2005, A&A, 435, 421
- Guetta, D., Spada, M., & Waxman, E. 2001, ApJ, 557, 399
- Ghirlanda, G., Ghisellini, G., & Celotti, A. 2004, A&A, 422, L55
- Hjorth, J., Sollerman, J., et al. 2005, ApJ, 630, L117
- Janka, H.-T., Eberl, T., Ruffert, M., & Fryer, C. L. 1999, ApJ, 527, L39
- Janka, H.-T. & Ruffert, M. 2002, in ASP Conference Series, Vol. 263, Stellar Collisions, Mergers and their Consequences, ed. M. M. Shara, 333
- Kobayashi, S., Piran, T., & Sari, R. 1997, ApJ, 490, 92
- Krimm, H., et al. 2005, GCN Circular N. 3667
- Liang, E.W., et al. 2006, ApJ, submitted (astro-ph/0602142)
- Mészáros, P. 2002, Ann. Rev. Astron. Astroph., 40, 137
- Nakar, E., & Piran, T. 2002, ApJ, 572, L139
- Nakar, E., Gal-Yam, A., & Fox, D. B. 2005 (astro-ph/0511254)
- Paczyński, B. 1986, ApJ, 308, L43
- Piran, T. 2005, Rev. Mod. Phys., 76, 1143
- Ramirez-Ruiz, E., Lloyd-Ronning, N.M. 2002, New Astronomy, 7, 197
- Rybicki, G. B., & Lightman, A. 1985, Radiative processes in astrophysics, Wiley (New York).
- Ruffert, M. & Janka, H.-T. 1999, A&A, 344, 573

- Sari, R., & Piran, T. 1997, ApJ, 485, 270
- Sato, G., et al. 2005, GCN Circular N. 3793
- Setiawan, S., Ruffert, M., & Janka, H.-T. 2004, MNRAS, 352, 753
- Soderberg, A. M., Berger, E., et al. 2006, (astro-ph/0601455)
- Tutukov, A.V., Yungelson, L.R., 1994, MNRAS268, 871
- Zhang, B., & Mészáros, P. 2002, ApJ, 581, 1236
- Zhang, B., et al. 2005, ApJ, in press (astro-ph/0508321)

Table 1: Observed short GRBs with determined redshifts.

GRB ^a	z	Band keV	T_{ob}^{b} ms	T_{i}^{c} ms	Fluence 10^{-8} erg cm ⁻²	$E_{\gamma,\text{iso}}^{\text{d}}$ 10^{50} erg	$\langle L \rangle^{\text{e}}$ 10^{50} erg s ⁻¹	E_{p} keV	η^{f}	k^{g}	Gal.	d^{h} kpc	SFR $M_{\odot} \text{ yr}^{-1}$	Ref. ⁱ
050509b	0.225	15–150	40	33	0.95 ± 0.25	0.011	0.8–1.5	> 150	1.5 ± 0.4	2.3–4.3	Ell	40	< 0.1	1,5
050709	0.16	30–400	70	60	29 ± 4	0.167	4.7	83_{-12}^{+18}	0.7 ± 0.2	1.7	SF	3.8	0.2	2,6
050724 ^j	0.257	15–350	250	200	11.3 ± 8.7	0.174	1.4–1.7	> 350	1.7 ± 0.2	1.6–1.9	Ell	2.6	< 0.02	3,7
			3000	2387	63 ± 10	0.97	0.7–0.8	...						
050813	0.722	15–350	600	350	12.4 ± 4.6	1.6	7.8–13	> 350	1.2 ± 0.3	1.7–2.8	?	–	–	4,8
051221	0.546	20–2000	1400	906	$320_{-1.7}^{+0.1}$	24	26	400 ± 80	–	1.0	SF	0.8	1.5	9

^a All the events were detected by Swift except GRB 050709, which was observed by HETE-2.

^b Observed duration T_{90} .

^c Intrinsic duration (cosmologically corrected).

^d Isotropic equivalent gamma-ray energy released by the burst in the specified band (cosmologically corrected).

^e Average luminosity (computed as $\langle L \rangle \equiv k E_{\gamma,\text{iso}}/T_{\text{i}}$).

^f Photon index of the average GRB spectrum ($f(E) \propto E^{-\eta}$).

^g Bolometric corrections to rest-frame energies of 20–2000 keV, following Bloom et al. (2001).

^h Projected distance of GRB from host center.

ⁱ References: 1. Gehrels et al. (2005); 2. Boer et al. (2005); 3. Krimm et al. (2005); 4. Sato et al. (2005);

5. Bloom et al. (2005); 6. Fox et al. (2005); 7. Berger et al. (2005); 8. Foley et al. (2005); 9. Soderberg et al. (2006).

^j This GRB shows a first short pulse, followed by a softer and longer event. We report data for both events.

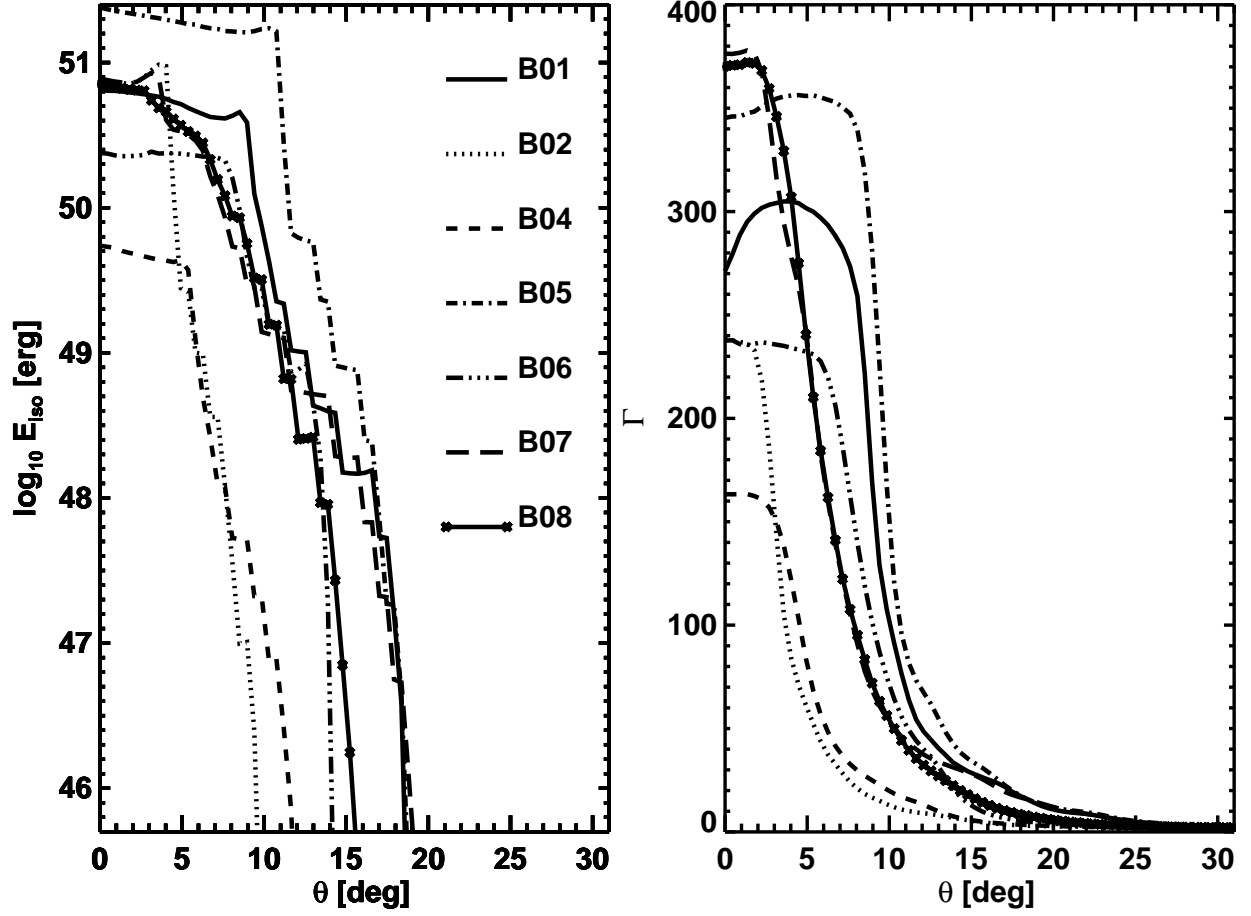


Fig. 1.— Properties of relativistic outflows from BH-torus systems as functions of viewing angle, determined by hydrodynamic simulations which show that collimated, ultrarelativistic mass ejection can be driven by sufficiently powerful deposition of thermal energy around the relic BH-torus systems of NS+NS/BH mergers. models B01–B08 differ in the rate of energy deposition per unit solid angle around the BH (AJM05). *Left*: Total (internal plus kinetic) isotropic equivalent energy of matter with terminal Lorentz factors $\Gamma_{\infty} > 100$. This energy may be larger than the GRB energy by a factor depending on the efficiency of conversion of outflow energy to γ -rays. *Right*: Radially averaged Lorentz factor Γ at 0.5 seconds after the onset of energy deposition (AJM05). Note that the terminal value Γ_{∞} can be higher by a factor of 2–3.

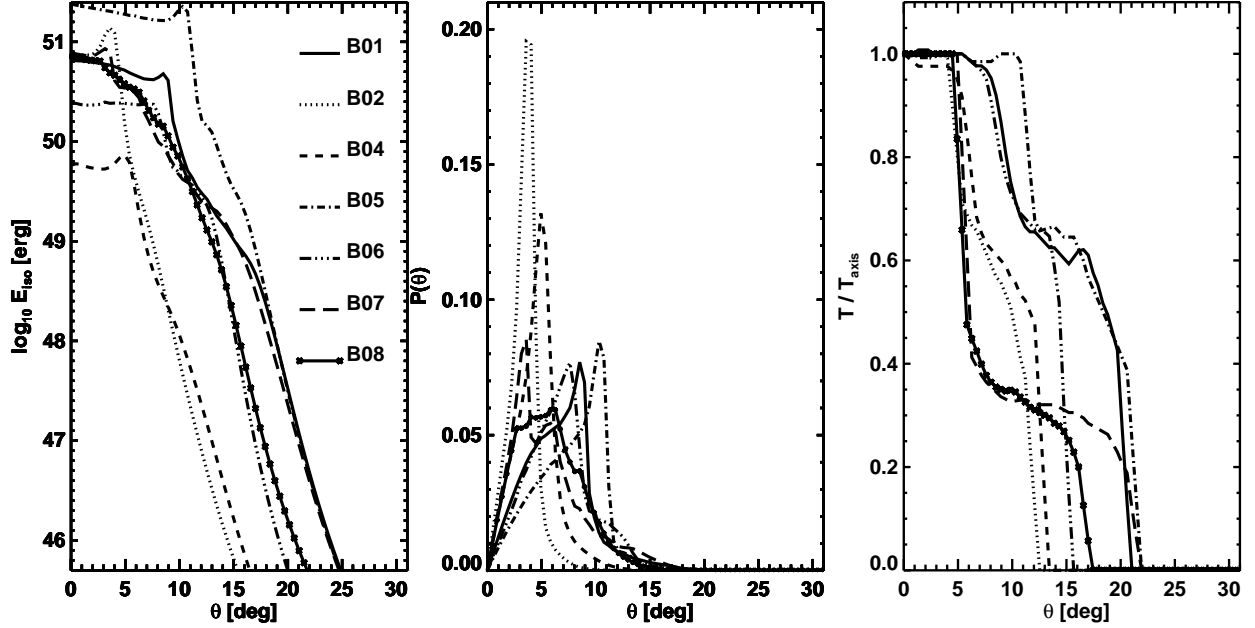


Fig. 2.— Observationally relevant properties of relativistic outflows from BH-torus systems as functions of viewing angle, calculated using the results of the hydrodynamic models of Fig. 1. *Left:* Total energy potentially radiated from ultrarelativistic, collimated ejecta with terminal Lorentz factors $\Gamma_{\infty} > 100$, including the contributions from matter moving not along the line of sight (see text for details). The main difference compared to the left panel in Fig. 1 is a smoothing of the jet wings and a slight widening at energies below about 10^{49} erg. *Middle:* Relative observability of short GRBs from different viewing angles, estimated according to Eq. (2), using the E_{iso} -values shown in the left panel. *Right:* Timescale of the observable GRB, estimated from the polar-angle dependent radial length $\Delta(\theta)$ of the ultrarelativistic outflow with $\Gamma_{\infty} > 100$ in the observer frame, relative to the on-axis duration.

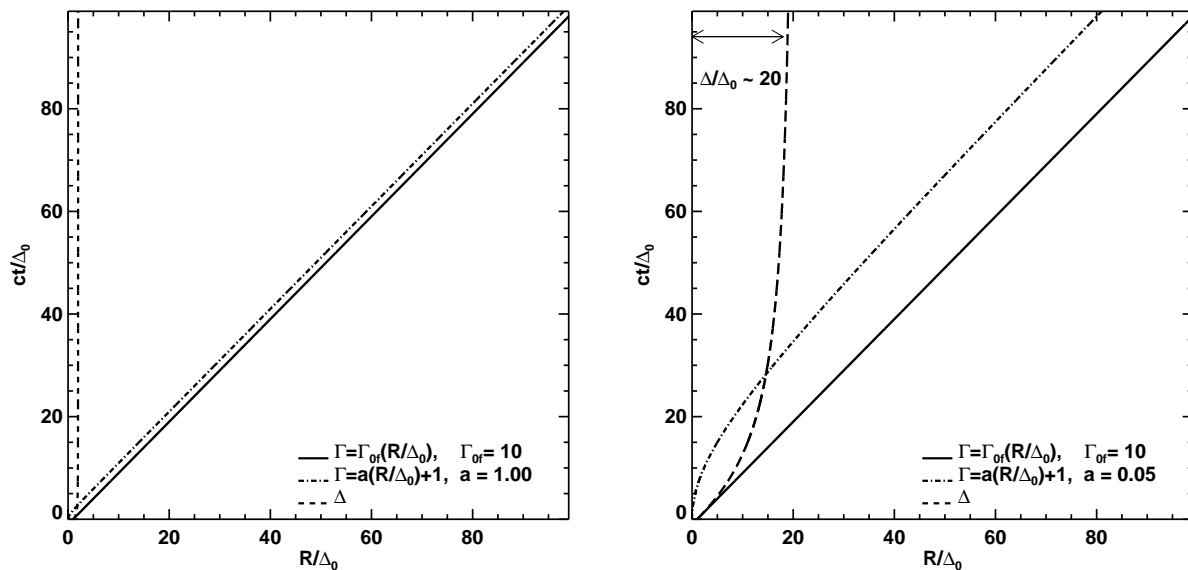


Fig. 3.— World-line diagrams for the evolution of shells at the forward and rear edges of the ultimately highly relativistic ejecta. While in the plot on the left the Lorentz factor is assumed to increase linearly and very quickly with distance from the source for both the leading and lagging shells, the plot on the right displays a situation that fits better the results of the hydrodynamic simulations of jet formation: The lagging shell accelerates more slowly than the leading one. The acceleration laws are indicated in the lower right corners of the two panels. Time $t = 0$ is the moment when the shell at the rear edge of the ejecta is born, and $\Delta_0 = ct_{ce}$ is the radial extension of the outflow at this time, when t_{ce} is the period of activity of the central engine. All lengths are normalized to Δ_0 . In the figure on the left the radial thickness of the expanding shell nearly saturates at a value of about $2\Delta_0$, whereas on the right one can see a stretching of the fireball compared to its initial length by roughly a factor of 20, before a much slower growth indicates a nearly saturated state. The parameters for this plot were chosen to closely reproduce the results of one of the jet models of AJM05.

